



## Synthesize of Cu<sub>2</sub>O-CuO/Sr<sub>3</sub>BiO<sub>5.4</sub> and its photocatalytic activity

Wei Zhao<sup>a,b</sup>, Kin-Hang Wong<sup>a</sup>, Chun Hu<sup>c</sup>, Jimmy C. Yu<sup>d,e</sup>, Chiu-Yeung Chan<sup>f</sup>, Tao Qi<sup>b,\*</sup>,  
Po-Keung Wong<sup>a,e,\*\*</sup>

<sup>a</sup> Department of Biology, The Chinese University of Hong Kong, Shatin, N.T., Hong Kong SAR, China

<sup>b</sup> Institute of Process Engineering, Chinese Academy of Sciences, Beijing 100190, China

<sup>c</sup> Research Center for Eco-Environmental Sciences, Chinese Academy of Sciences, Beijing 100085, China

<sup>d</sup> Department of Chemistry, The Chinese University of Hong Kong, Shatin, N.T., Hong Kong SAR, China

<sup>e</sup> Environmental Science Programme, The Chinese University of Hong Kong, Shatin, N.T., Hong Kong SAR, China

<sup>f</sup> Department of Microbiology, The Chinese University of Hong Kong, Shatin, N.T., Hong Kong SAR, China

### ARTICLE INFO

#### Article history:

Received 1 August 2011

Received in revised form

25 November 2011

Accepted 25 November 2011

Available online 2 December 2011

#### Keywords:

Photocatalysts

Visible light

Copper

Disinfection

Degradation

### ABSTRACT

A visible-light-driven photocatalyst, Cu<sub>2</sub>O-CuO/Sr<sub>3</sub>BiO<sub>5.4</sub>, was synthesized by the precipitation method using a new acidic system with basic ethylenediamine tetraacetic acid disodium salt (Na<sub>2</sub>EDTA) as the buffer reagent. Part of Cu<sub>2</sub>O was formed on the surface of Sr<sub>3</sub>BiO<sub>5.4</sub> *in situ* during the calcination. 5.4 log inactivation of *Escherichia coli* K-12 and 27% degradation of naphthalene were achieved in 3 and 2 h, respectively, under the visible light irradiation provided by fluorescent lamps. The results of this study suggested that Cu<sub>2</sub>O-CuO on the surface of Sr<sub>3</sub>BiO<sub>5.4</sub> is stable and can effectively promote the visible light photocatalytic activity of Sr<sub>3</sub>BiO<sub>5.4</sub>.

© 2012 Published by Elsevier B.V.

### 1. Introduction

Titanium dioxide (TiO<sub>2</sub>) is the most commonly used photocatalyst due to its high photocatalytic activity, non-toxic and chemical stability under the UV irradiation [1]. In order to expand its photoactivity to the visible light (VL) region, which is the main part of sunlight, many approaches have been attempted. These approaches include doping transition metals into TiO<sub>2</sub> [2], generating reduced TiO<sub>x</sub> [3] and doping the non-metal elements into TiO<sub>2</sub> [4]. However, due to the limitation of the light absorption characterization of TiO<sub>2</sub>-based photocatalyst, their photocatalytic efficiencies are still undesirable under VL irradiation. Thus, developing a new type visible-light-driven (VLD) catalyst with high photocatalytic efficiency under VL is needed. Because of the deep valence bands of metal oxide formed by O<sub>2p</sub>, if the conduction band is moved down to reduce the band gap, the reduced conduction band level is easily below the potential level of O<sub>2</sub>/<sup>•</sup>O<sub>2</sub><sup>-</sup> (superoxide) (-0.56 V vs standard hydrogen electrode (SHE), pH=0), then, the forma-

tion of reactive oxidative species (e.g. <sup>•</sup>O<sub>2</sub><sup>-</sup>) will not be possible [5]. Thus, one of reasonable approaches for developing new VLD photocatalysts is to find some elements with the orbital that can control the valence band besides the O<sub>2p</sub>. In 1999, Kudo et al. [6] found the valence band (Bi<sup>5+</sup>/Bi<sup>3+</sup>) of Bi<sub>6s</sub> can be adjusted slightly higher than that of O<sub>2p</sub>, then the valence band controlled by the Bi<sub>6s</sub> or the hybrid Bi<sub>6s</sub>-O<sub>2p</sub> orbital can be formed. Later, Shimodaira et al. [7] found that a layered structure of bismuth mixed oxides can promote the generation and separation of the charge carriers; and can decrease the recombination between the photogenerated electrons and holes. Based on these observations, Tang et al. [8] and Hu et al. [9] developed two highly efficient VLD photocatalyst, namely, CaBi<sub>2</sub>O<sub>4</sub> and NiO/SrBi<sub>2</sub>O<sub>4</sub>, to decompose organic contaminants and disinfect bacteria, respectively. However, in their studies, the calcination conditions were very harsh (calcined at 350 °C for 10 h and then calcined at 800 °C for 12 h) and an expensive Xenon lamp was used to provide VL light. These stringent requirements probably render their practice application. In addition, in their H<sub>2</sub>O-ethylenediaminetetraacetic acid (EDTA)-ammonia (NH<sub>3</sub>·H<sub>2</sub>O)-citric acid (CA) buffer system, the coprecipitation behavior of metal precursors could not be controlled conveniently. In this study, basic ethylenediaminetetraacetic acid disodium salt (Na<sub>2</sub>EDTA) was used to replace the acidic EDTA as the buffer reagent and synthesized the Sr<sub>3</sub>BiO<sub>5.4</sub> metal oxide under a HNO<sub>3</sub>-Na<sub>2</sub>EDTA-NH<sub>3</sub>·H<sub>2</sub>O-CA buffer system. By calcining the Cu

\* Corresponding author.

\*\* Corresponding author at: Department of Biology, The Chinese University of Hong Kong, Shatin, N.T., Hong Kong SAR, China. Tel.: +86 852 2609 6383; fax: +86 852 2603 5767.

E-mail addresses: [tqi@home.ipe.ac.cn](mailto:tqi@home.ipe.ac.cn) (T. Qi), [pkwong@cuhk.edu.hk](mailto:pkwong@cuhk.edu.hk) (P.-K. Wong).

loaded  $\text{Sr}_3\text{BiO}_{5.4}$  precursors only at  $300^\circ\text{C}$  for 1 h, we obtained the highly effective VLD photocatalysts,  $\text{Cu}_2\text{O-CuO/Sr}_3\text{BiO}_{5.4}$ . This new VLD photocatalyst showed good performance for the disinfection of *Escherichia coli* K-12 and degradation of naphthalene under the VL irradiation provided by fluorescent lamps.

## 2. Experimental

### 2.1. Preparation of photocatalysts

#### 2.1.1. Preparation of $\text{Sr}_3\text{BiO}_{5.4}$

Stoichiometric amounts of  $\text{Sr}(\text{NO}_3)_2$  and  $\text{Bi}(\text{NO}_3)_3 \cdot 5\text{H}_2\text{O}$  were dissolved in the mixture of  $\text{HNO}_3$  and deionized water, and a solution of  $\text{Na}_2\text{EDTA}$  in ammonia and citric acid was added into the above solution. During this process, the mixed solution was stirred continuously. Then, ammonia was added to adjust pH until a white precipitate was formed. The precipitate was filtered and dried at  $140^\circ\text{C}$  to remove water and obtain the  $\text{Sr}_3\text{BiO}_{5.4}$  precursor. After calcining this precursor at  $300^\circ\text{C}$  ( $2^\circ\text{C min}^{-1}$ ) in air for 1 h,  $\text{Sr}_3\text{BiO}_{5.4}$  sample was obtained.

#### 2.1.2. Preparation of $\text{Cu}_2\text{O-CuO/Sr}_3\text{BiO}_{5.4}$ , $\text{CuO/P25}$ and $\text{CuO/Sr}_3\text{BiO}_{5.4}$

0.5 g sample ( $\text{Sr}_3\text{BiO}_{5.4}$  precursor; P25 (Degussa:Hulls);  $\text{Sr}_3\text{BiO}_{5.4}$ ) was immersed into 2 mL of 0.1 M  $\text{Cu}(\text{NO}_3)_2$  aqueous solution and evaporated at  $60^\circ\text{C}$  by stirring. The final dried powder was calcined at  $300^\circ\text{C}$  in air for 1 h.

$\text{CuO}$  was prepared directly by calcining the  $\text{Cu}(\text{NO}_3)_2$  at  $300^\circ\text{C}$  ( $2^\circ\text{C min}^{-1}$ ) for 1 h.  $\text{Cu}_2\text{O}$  was purchased from Sigma company.

### 2.2. Physicochemical characterization of photocatalysts

X-ray diffraction (XRD) of  $\text{Cu}_2\text{O-CuO/Sr}_3\text{BiO}_{5.4}$  was recorded on a Bruker AXS D8 advance diffractometer with  $\text{Cu K}\alpha$  radiation ( $\lambda = 1.54059 \text{ \AA}$ ). The TEM images were obtained from a CM-120 (Philips) transmission electron microscope operated at 120 kV. UV-vis absorption spectra of the samples were recorded by a UV-vis spectrophotometer (Hitachi UV-3100) with an integrated sphere attachment. The X-ray photoelectron spectroscopy (XPS) data was recorded by a Quantum 2000 scanning ESCA microprobe instrument ( $\Phi$  Physical Electronics) using monochromatic  $\text{Al K}\alpha$  radiation (225 W, 15 mA, 15 kV) with the spot size of  $100 \mu\text{m}$  and low-energy electron flooding for charge compensation. To compensate surface charges effects, binding energies were calibrated using the  $\text{C}_{1s}$  hydrocarbon peak at 284.5 eV. Concentrations of metal ions was measured by a Hitachi Z8100 polarized Zeeman atomic absorption spectrophotometer.

### 2.3. Photocatalytic reactions

$0.1 \text{ g L}^{-1}$  photocatalyst was added into 50 mL diluted *E. coli* K-12 suspension. The light source was provided by six fluorescent lamps with a total light intensity of  $10.5 \text{ mW cm}^{-2}$ . Light passed through a liquid filter with 0.2 M  $\text{NaNO}_2$  solution to cut off UV ( $\lambda < 420 \text{ nm}$ ). The reaction temperature was maintained at  $25^\circ\text{C}$ . A bacterial suspension without photocatalyst was irradiated as a light control, while the reaction mixture with no irradiation was included as a dark control. Before and during the irradiation, an aliquot of the reaction solution was sampled and immediately diluted with sterilized saline (0.9% NaCl) solution. 0.1 mL of the diluted sample was spread on nutrient agar plate and incubated at  $37^\circ\text{C}$  for 20 h. The colonies were counted to determine the number of viable cells.

50 mL aqueous suspensions of naphthalene ( $10 \text{ mg L}^{-1}$ ) and 25 mg of photocatalyst powders were placed in a 125 mL beaker. Prior to irradiation, the suspensions were magnetically stirred in dark for 30 min to establish adsorption/desorption equilibrium

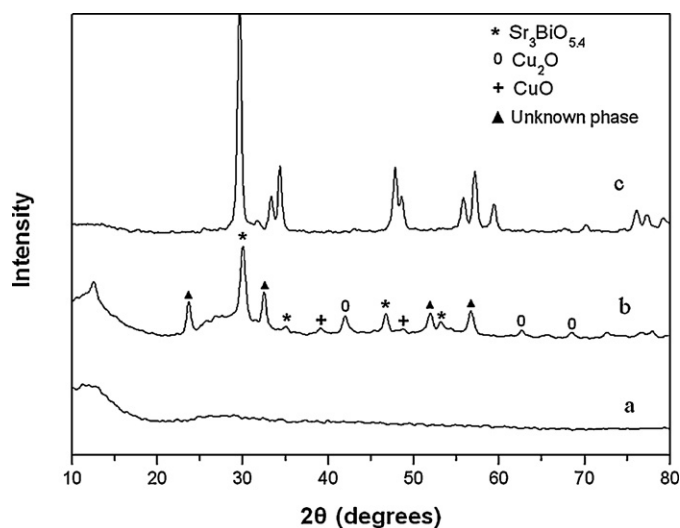


Fig. 1. XRD pattern of different samples. (a) As-synthesized  $\text{Cu}_2\text{O-CuO/Sr}_3\text{BiO}_{5.4}$ , (b)  $\text{Cu}_2\text{O-CuO/Sr}_3\text{BiO}_{5.4}$  and (c)  $\text{Sr}_3\text{BiO}_{5.4}$ .

between the naphthalene and the surface of the photocatalyst at  $25^\circ\text{C}$ . At given irradiation time intervals, 3 mL aliquots were collected, centrifuged, and then filtered. The filtrates were extracted by hexane, and then analyzed by an Agilent 6890 gas chromatograph equipped with a HP-5 MS capillary column and a flame ionization detector.

## 3. Results and discussions

Fig. 1 shows the XRD pattern of different  $\text{Sr}_3\text{BiO}_{5.4}$  samples. For the as-synthesized  $\text{Cu}_2\text{O-CuO/Sr}_3\text{BiO}_{5.4}$  sample (Fig. 1a), the spectra show an amorphous phase with two weak peaks at  $11.2^\circ$  and  $27.4^\circ$ , respectively. These results indicate that the precursors of bismuth and strontium have a initial arrangement since  $\text{Bi}(\text{NO}_3)_3 \cdot 5\text{H}_2\text{O}$  has a better solubility in acidic medium and EDTA- $\text{Na}_2\text{EDTA}$  buffer reagent is more beneficial to control pH than EDTA itself in the acid-base system. For the  $\text{Cu}_2\text{O-CuO/Sr}_3\text{BiO}_{5.4}$  sample (Fig. 1b), the peaks of  $30.1^\circ$ ,  $35.5^\circ$ ,  $47.2^\circ$ , and  $53.5^\circ$  correspond to the monoclinic system of  $\text{Sr}_3\text{BiO}_{5.4}$  crystallized in a layered crystal structure. The weak peaks of  $42.5^\circ$ ,  $62.6^\circ$ , and  $72.7^\circ$  belong to  $\text{Cu}_2\text{O}$ , while other two comparatively weak peaks of  $38.8^\circ$  and  $48.7^\circ$  indicate the presence of  $\text{CuO}$ . There are no signals of  $\text{Cu}^0$  and copper hydroxides appearing in this pattern since the copper hydroxides were decomposed completely and  $\text{Cu}^0$  did not formed under these calcining conditions. The low peak intensity of  $\text{Cu}_2\text{O}$  and  $\text{CuO}$  is caused by low contents or forming the fine particles. Besides above peaks, there are four peaks at  $23.7^\circ$ ,  $32.6^\circ$ ,  $52.0^\circ$  and  $56.7^\circ$  that the software could not check out. By comparing these peaks to the XRD pattern of  $\text{Sr}_3\text{BiO}_{5.4}$  sample (Fig. 1c),  $32.6^\circ$  and  $56.7^\circ$  two peaks can be attributed to this sample. Thus, we speculated the unknown phase probably will be the mixture of other strontium bismuth oxide component.

Fig. 2 shows the TEM images of  $\text{Cu}_2\text{O-CuO/Sr}_3\text{BiO}_{5.4}$ . The sample is composed of the irregular small particles with the size between 200 and 300 nm (Figs. 2a–c). Sometimes, these particles aggregate to form larger particles (Fig. 2d). The selective area electron diffraction (ED) pattern of an individual particle (the inset of Fig. 2c) shows that the well-defined ED spots indicating the crystal nature of the particle. There is no appearance of  $\text{Cu}_2\text{O}$  or  $\text{CuO}$  particle. This result agrees with the XRD result that  $\text{Cu}_2\text{O/CuO}$  exists as fine particles.

The UV-vis absorption spectra of the  $\text{Cu}_2\text{O-CuO/Sr}_3\text{BiO}_{5.4}$  together with others are shown in Fig. 3. For the Cu loaded  $\text{Sr}_3\text{BiO}_{5.4}$  precursors sample, there is a strong absorption peak at 248 nm

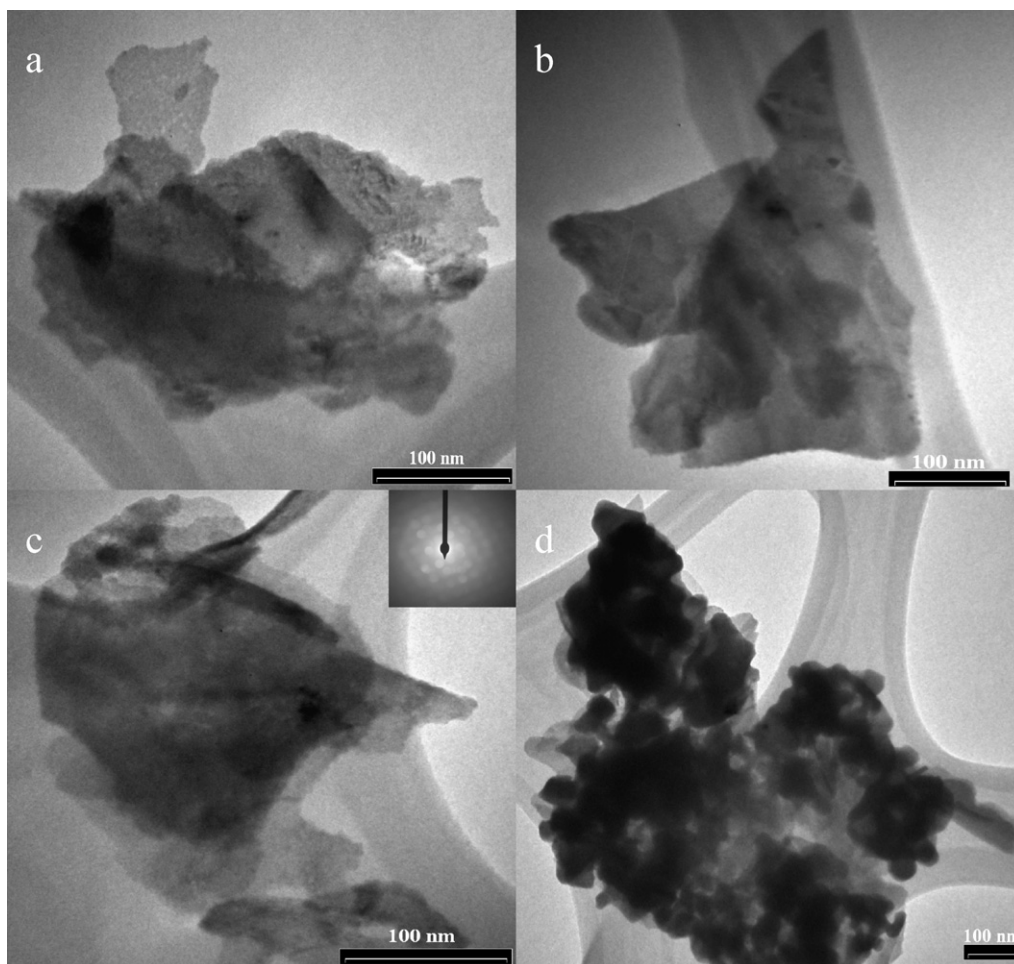


**Fig. 2.** The TEM images of  $\text{Cu}_2\text{O-CuO/Sr}_3\text{BiO}_{5.4}$ . (a), (b) and (c) are the images of different particles. The inset of image (c) is the electron diffraction (ED) pattern of this particle. (d) The image of the particles in low resolution.

(Fig. 3a), while there is no absorption at 420–550 nm region since neither  $\text{Cu}_2\text{O/CuO}$  nor the monoclinic system of  $\text{Sr}_3\text{BiO}_{5.4}$  was formed at that time. After calcination, the absorption spectrum of this sample changes significantly (Fig. 3c). It shows that the

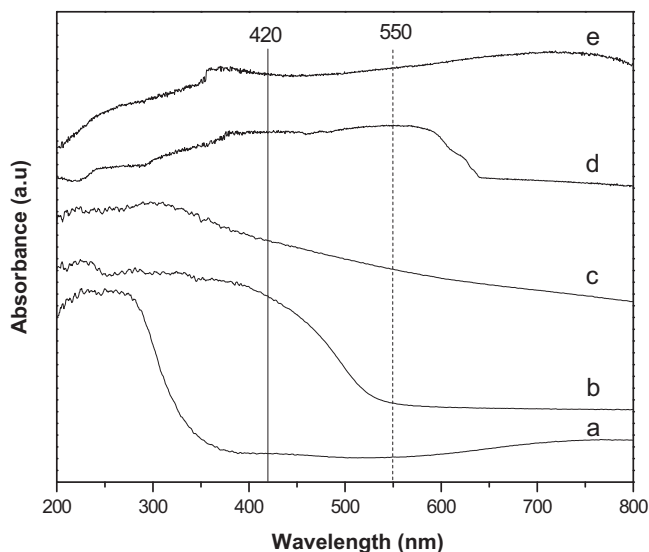


**Fig. 3.** UV-vis diffuse reflectance spectra of different samples. (a) Cu load  $\text{Sr}_3\text{BiO}_{5.4}$  precursors, (b)  $\text{Sr}_3\text{BiO}_{5.4}$ , (c)  $\text{Cu}_2\text{O-CuO/Sr}_3\text{BiO}_{5.4}$ , (d)  $\text{Cu}_2\text{O}$  and (e)  $\text{CuO}$ .

UV-vis absorption shifts to the long wavelength direction and the absorption peak spreads across the whole VL absorption band (420–700 nm). Based on the absorption spectra of  $\text{Sr}_3\text{BiO}_{5.4}$  (Fig. 3b) and  $\text{Cu}_2\text{O}$  (Fig. 3d), we found both of them can absorb the VL (420–550 nm). Moreover, the absorption spectra of  $\text{Cu}_2\text{O}$  even extend its absorption to 642 nm. This result suggests that  $\text{Cu}_2\text{O-CuO/Sr}_3\text{BiO}_{5.4}$  probably has good photocatalytic ability under the VL irradiation by the fluorescent lamps (there are two peak (550 nm and 620 nm) with very high intensity (4000 counts) in the spectrum of Fluorescent lamp, Supporting file Fig. 1).

In order to investigate the Cu species on the surface of different photocatalysts, XPS measurements were performed (Fig. 4). For the  $\text{CuO/TiO}_2$  (Fig. 4c) and  $\text{CuO/Sr}_3\text{BiO}_{5.4}$  (Fig. 4d), there is a symmetrical peak emerged at 933.6 eV in the slow scanning spectrum of  $\text{Cu}2p_{3/2}$ , which value is same as that of the pure  $\text{CuO}$  (Fig. 4b). These results suggest that  $\text{CuO}$  is present solely on the surface of these two photocatalysts. For the  $\text{Cu}_2\text{O-CuO/Sr}_3\text{BiO}_{5.4}$ , an asymmetrical peak appears around 932.4 eV, which value is between those of pure  $\text{CuO}$  and  $\text{Cu}_2\text{O}$  (Fig. 4a). After deconvolution, this peak is divided into two peaks of 931.6 and 933.6 eV (the inset of Fig. 4), which are corresponding to the signals of  $\text{Cu}_2\text{O}$  and  $\text{CuO}$ , respectively. It means both  $\text{CuO}$  and  $\text{Cu}_2\text{O}$  are present on the surface of this photocatalyst. The reason for the formation of  $\text{Cu}_2\text{O}$  probably is that the  $\text{Cu}(\text{NO}_3)_2$  is loaded on the  $\text{Sr}_3\text{BiO}_{5.4}$  precursors. During the calcinations, the C or CO which comes from the uncompleted combustion of organic compound(s) (such as  $\text{Na}_2\text{EDTA}$  and citric acid) can reduce  $\text{CuO}$  to  $\text{Cu}_2\text{O}$ .

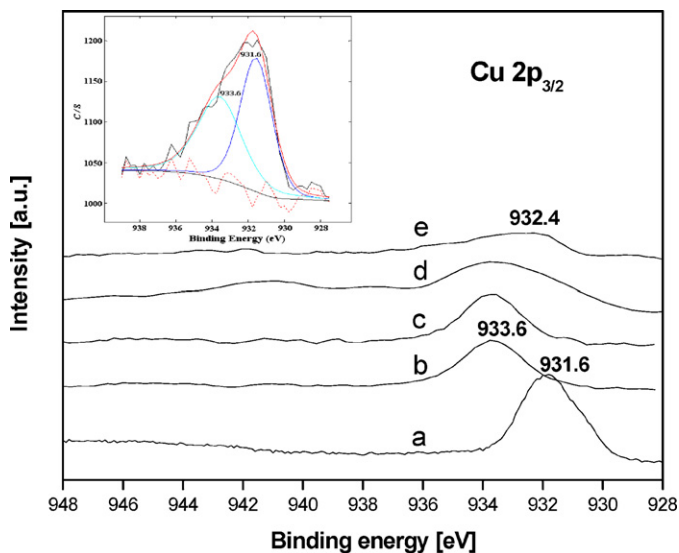


**Fig. 4.** The XPS spectra of different photocatalysts. (a)  $\text{Cu}_2\text{O}$ , (b)  $\text{CuO}$ , (c)  $\text{CuO}/\text{P25}$ , (d)  $\text{CuO}/\text{Sr}_3\text{BiO}_{5.4}$  and (e)  $\text{Cu}_2\text{O}-\text{CuO}/\text{Sr}_3\text{BiO}_{5.4}$ . The inset is the deconvolution result of 932.4 eV peak appearing in spectra (e).

5.4 log of *E. coli* K-12 is inactivated within 3 h in  $\text{Cu}_2\text{O}-\text{CuO}/\text{Sr}_3\text{BiO}_{5.4}$  suspension under VL irradiation provided by the fluorescent lamps (Fig. 5f). Light control result (Fig. 5a) suggests VL provided by fluorescent lamps have no significant bactericidal effects on *E. coli* K-12 (only 0.03 log inactivation). The  $\text{Sr}_3\text{BiO}_{5.4}$  does not show any significant VL bacterial inactivation (only 0.18 log inactivation, Fig. 5c) since the VL intensity of fluorescent lamps is weak in 420–550 nm region (Supporting file Fig. 1) which it can absorb. The dark reaction of  $\text{Cu}_2\text{O}-\text{CuO}/\text{Sr}_3\text{BiO}_{5.4}$  shows some bactericidal activity (1.24 log inactivation) (Fig. 5b). These results indicate the photocatalyst itself is slightly toxic to *E. coli* K-12. For  $\text{CuO}/\text{Sr}_3\text{BiO}_{5.4}$  (Fig. 5d) and  $\text{CuO}/\text{P25}$  (Fig. 5e), the VL bacterial inactivation is 0.91 and 0.7 log, respectively. It is interesting to notice that the VL bactericidal effect of  $\text{CuO}/\text{Sr}_3\text{BiO}_{5.4}$  is very close to the sum of those of  $\text{Sr}_3\text{BiO}_{5.4}$  and  $\text{CuO}/\text{P25}$ . Since the P25 cannot absorb

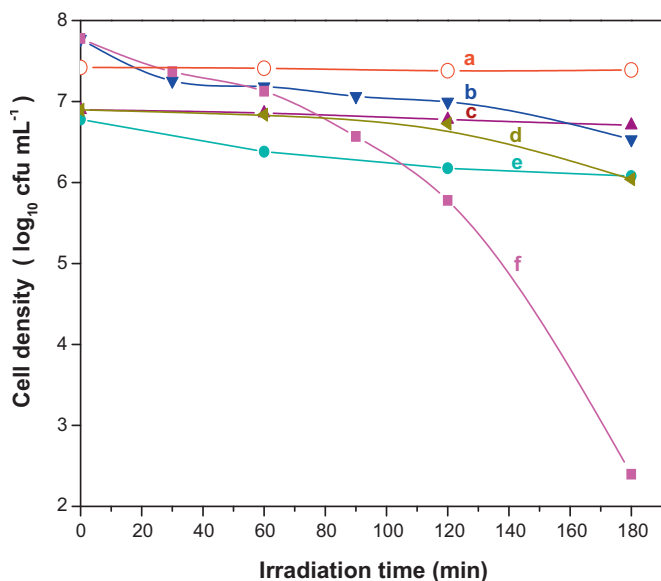


**Fig. 5.** Inactivation of *E. coli* K-12 in the presence of various photocatalysts. (a) Light control, (b) dark control of  $\text{Cu}_2\text{O}-\text{CuO}/\text{Sr}_3\text{BiO}_{5.4}$ , (c) light reaction of  $\text{Sr}_3\text{BiO}_{5.4}$ , (d) light reaction of  $\text{CuO}/\text{Sr}_3\text{BiO}_{5.4}$ , (e) light reaction of  $\text{CuO}/\text{P25}$  and (f) light reaction of  $\text{Cu}_2\text{O}-\text{CuO}/\text{Sr}_3\text{BiO}_{5.4}$ .

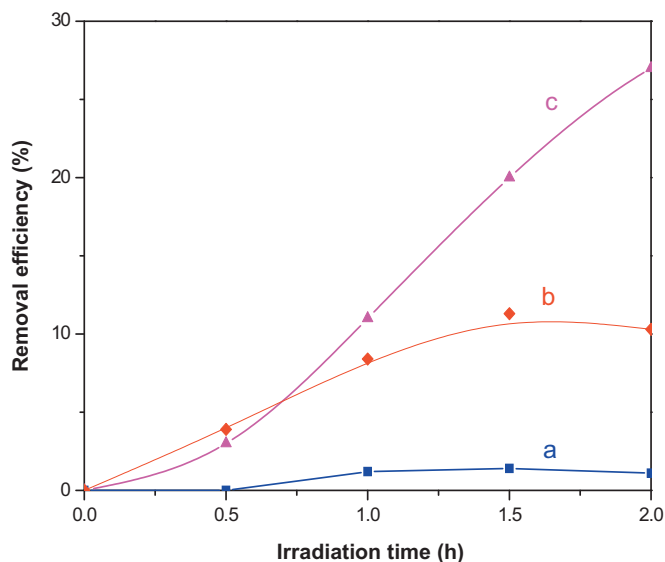


**Fig. 6.** Photocatalytic decomposition of naphthalene over  $\text{Cu}_2\text{O}-\text{CuO}/\text{Sr}_3\text{BiO}_{5.4}$ . (a) Light control, (b) dark reaction and (c) PCO reaction.

VL, one can assign 0.91 log inactivation into: (1) 0.18 log inactivation from  $\text{Sr}_3\text{BiO}_{5.4}$  and (2) 0.7 log inactivation from  $\text{CuO}$  under VL irradiation. Also, this result suggests that  $\text{CuO}$  cannot effectively enhance the photocatalytic activity of  $\text{Sr}_3\text{BiO}_{5.4}$  under VL irradiation provided by the fluorescent lamps.

Due to the poor VL bacterial inactivation of  $\text{Sr}_3\text{BiO}_{5.4}$  itself (0.18 log inactivation), surface Cu species play the key role to cause the large activity difference between  $\text{Cu}_2\text{O}-\text{CuO}/\text{Sr}_3\text{BiO}_{5.4}$  and  $\text{CuO}/\text{Sr}_3\text{BiO}_{5.4}$ . Further, we measured the concentration of free  $\text{Cu}^{2+}$  during the photocatalytic bactericidal experiment. The concentration of free  $\text{Cu}^{2+}$  in the solution was almost unchanged (from 7.7  $\mu\text{M}$  at 0 h to 7.8  $\mu\text{M}$  at 3 h). It means the  $\text{Cu}_2\text{O}/\text{CuO}$  on the surface of  $\text{Sr}_3\text{BiO}_{5.4}$  was relatively stable under these reaction conditions (Actually, the  $\text{Cu}_2\text{O}-\text{CuO}/\text{Sr}_3\text{BiO}_{5.4}$  catalyst still keeps its 80% activity after five times reused) and a homogeneous Fenton-like reaction induced by the dissolved  $\text{Cu}_2\text{O}$  or  $\text{CuO}$  did not occur. Since  $\text{Cu}_2\text{O}$  can absorb large amount of different oxygen species ( $\text{O}_2$ ,  $\text{O}^-$  and  $\cdot\text{O}_2^-$ ) and possesses a strong ability to reduce  $\text{O}_2$  [10,11], we believe this property of  $\text{Cu}_2\text{O}$  will be of advantage for it to trap the electron(s). In addition, the absorption spectrum of  $\text{Cu}_2\text{O}-\text{CuO}/\text{Sr}_3\text{BiO}_{5.4}$  sample (Fig. 3c) shows that it can absorb VL even up to the region of 700 nm. It means this photocatalyst can generate more photogenerated charge carrier number, and lead to a better PCO activity. Of course, the toxicity of  $\text{Cu}_2\text{O}-\text{CuO}$  enhanced by the photogenerated charge carriers ( $\text{h}^+$  and  $\text{e}^-$ ) from  $\text{Sr}_3\text{BiO}_{5.4}$  (even the unknown phase) under VL irradiation, the synergistic inactivation between the toxicity of  $\text{Cu}_2\text{O}-\text{CuO}$  and the enhanced photocatalytic activity of  $\text{Sr}_3\text{BiO}_{5.4}$  (This sample showed some photocatalytic degradation activity of Rhodamine B. Supporting file Fig. 2) by  $\text{Cu}_2\text{O}-\text{CuO}$  cannot be neglected. Further studies are required to assess the contribution of these factors.

The result of naphthalene (NAP) degradation (Fig. 6) also illustrates the good VL activity of this new photocatalyst. After 2 h VL irradiation ( $\lambda > 420$  nm) provided by the fluorescent lamps, 27% naphthalene had been degraded while NAP is not degraded in the absence of photocatalyst. The dark reaction result shows that there is a weak NAP adsorption onto surface of the photocatalyst. Because NAP did not show the self-photosensitized degradation, which frequent happens on the dye, thus, the photocatalytic process was the predominant process under these fluorescence lamp test conditions. In addition, since  $\text{Sr}_3\text{BiO}_{5.4}$  itself did not exhibit the photocatalytic activity for the decomposition of naphthalene under

fluorescence lamps we believed the  $\text{Cu}_2\text{O}$ - $\text{CuO}$  species play the key role for this photocatalytic process.

#### 4. Conclusions

The highly efficient VLD photocatalyst  $\text{Cu}_2\text{O}$ - $\text{CuO}/\text{Sr}_3\text{BiO}_{5.4}$  was prepared by an economic and convenient method. The results from both *E. coli* K-12 bacterial inactivation and NAP degradation indicate that this new photocatalyst has a good photocatalytic activity under VL irradiation provided by the fluorescence lamps. The nanometer-sized  $\text{Cu}_2\text{O}$  on the surface of  $\text{Sr}_3\text{BiO}_{5.4}$  plays an important role for increasing the photocatalytic activity of this photocatalyst. We believe that this VLD photocatalyst have a good performance in potential applications. More studies in this area are being conducted.

#### Acknowledgements

The project was supported by a research grant (CUHK4585/06M) of Research Grant Council, Hong Kong SAR Government, allocated to P.K. Wong, C. Hu, J.C. Yu and C.Y. Chan, both a research grant (51125018) from National Science Foundation for Distinguished

Young Scholars of China and a research grant (51090380) from the Major Program of the National Natural Science Foundation of China allocated to T. Qi.

#### Appendix A. Supplementary data

Supplementary data associated with this article can be found, in the online version, at doi:10.1016/j.apsusc.2011.11.112.

#### References

- [1] A. Fujishima, K. Honda, *Nature* 238 (1972) 37–38.
- [2] F.B. Li, X.Z. Li, *Chemosphere* 48 (2002) 1103–1108.
- [3] D.C. Cronemeyer, *Phys. Rev.* 113 (1959) 1222–1226.
- [4] R. Asahi, T. Morikawa, T. Ohwaki, K. Aoki, Y. Taga, *Science* 293 (2001) 269–271.
- [5] J.W. Tang, Z.G. Zou, J.H. Ye, *J. Phys. Chem. B* 107 (2003) 14265–14269.
- [6] A. Kudo, K. Omori, H. Kato, *J. Am. Chem. Soc.* 121 (1999) 11459–11467.
- [7] Y. Shimodaira, H. Kato, H. Kosayoshi, A. Kudo, *J. Phys. Chem. B* 110 (2003) 17790–17797.
- [8] J.W. Tang, Z.G. Zou, J.H. Ye, *Angew. Chem. Int. Ed.* 43 (2004) 4463–4466.
- [9] C. Hu, X.X. Hu, J. Guo, J.H. Qu, *Environ. Sci. Technol.* 40 (2006) 5508–5513.
- [10] J.L. Li, L. Liu, Y. Yu, Y.W. Tang, H.L. Li, F.P. Du, *Electron. Commun.* 6 (2004) 940–943.
- [11] Z.K. Zheng, B.B. Huang, Z.Y. Wang, M. Guo, X.Y. Qin, X.Y. Zhang, P. Wang, Y. Dai, *J. Phys. Chem. C* 113 (2009) 114448–114453.